Available online at www.sciencedirect.com
ScienceDirect
Advanced Drug Delivery Reviews 59 (2007) 1054–1068
Advanced DRUG DELIVERY Reviews
www.elsevier.com/locate/addr

Modeling oxaliplatin drug delivery to circadian rhythms in drug metabolism and host tolerance ☆

Jean Clairambault *

INSERM U 776 "Rythmes Biologiques et Cancers", Paul-Brousse Hospital, F9480 Villejuif, and INRIA Rocquencourt, Domaine de Voluceau, BP 105, F78153 Rocquencourt, France

Received 1 May 2006; accepted 25 August 2006
Available online 28 June 2007

Abstract

To make possible the design of optimal (circadian and other period) time-scheduled regimens for cytotoxic drug delivery by intravenous infusion, a pharmacokinetic–pharmacodynamic (PK–PD, with circadian periodic drug dynamics) model of chemotherapy on a population of tumor cells and its tolerance by a population of fast renewing healthy cells is presented. The application chosen for identification of the model parameters is the treatment by oxaliplatin of Glasgow osteosarcoma, a murine tumor, and the healthy cell population is the jejunal mucosa, which is the main target of oxaliplatin toxicity in mice. The model shows the advantage of a periodic time-scheduled regimen, compared to the conventional continuous constant infusion of the same daily dose, when the biological time of peak infusion is correctly chosen. Furthermore, it is well adapted to using mathematical optimization methods of drug infusion flow, choosing tumor population minimization as the objective function and healthy tissue preservation as a constraint. Such a constraint is in clinical settings tunable by physicians by taking into account the patient's state of health.

Keywords: Theoretical models; Cancer drug toxicity; Pharmacokinetics-pharmacodynamics; Treatment outcome; Chronotherapy; Drug-delivery optimization

Contents

☆ This review is part of the *Advanced Drug Delivery Reviews* theme issue on "Chronobiology, Drug Delivery and Chronotherapeutics".

* Tel.: +33 1 39 63 55 43; fax: +33 1 39 63 58 82.
E-mail address: jean.clairambault@inria.fr.

0169-409X/$ - see front matter © 2007 Elsevier B.V. All rights reserved.
doi:10.1016/j.addr.2006.08.004

1. Physiological and pharmacological background

1.1. Chronobiology and cancer chronotherapeutics

Circadian rhythms have long been known in animals and humans, and taken into account in the therapy of cancer in humans during the past 20 years by various teams of clinicians in Europe, China, Canada and the United States. Recently, molecular biology has brought new insight about the mechanisms by which such rhythms are generated [1–3]. New understanding has been realized at the molecular level revealing connections between circadian clocks and cancer therapeutics [4–6] (see also the review in [7] for a state-of-the-art in cancer chronotherapeutics).

Our goal here is to provide a tool that is applicable in clinical settings. Herein, we design a model depending on parameters that are identifiable, relying on experimental observations at the scale of the living organism, to yield a macroscopic representation of the evolution of cell populations exposed to cytotoxic drugs used in cancer therapeutics. Even though the model is clearly dedicated to cancer therapeutics, we wish to point out that its pharmacokinetic–pharmacodynamic (PK–PD) part originated primarily from models commonly used in antibiotherapy, and from more general chronophar-macological considerations, as described in [8]. Thus we believe that this model can be generalized to other medical fields.

1.2. Aims of this study

Various teams of oncologists worldwide now take into account the fact that for a given cytotoxic drug, improved anti-tumor efficacy and reduced toxicity are possible when delivered at a determined circadian time, depending on the particular drug used. This approach has led to significant improvements in life expectancy and quality, for example, in patients with colorectal cancer.

To our knowledge, there is no theoretical model as yet that explains or predicts the qualitative behavior of an organism undergoing different time-scheduled anti-tumor therapeutic regimens. The aim of this article is to partially fill this void, by providing physicians and drug-delivery scientists with a practical tool to enable them to improve the clinical efficacy of anti-tumor treatments while minimizing their toxic effects on healthy tissues by using optimally designed time-scheduled regimens.

Since time matters in *chronotherapeutics*, such a tool must be dynamic and be composed of PK–PD differential equations describing the observed chronosensitivity of tumor growth and healthy tissue homeostasis on a drug delivered by intravenous infusion, the flow of which (as a function of time) is the external control law to be optimized.

The six variables of the dynamic system considered here (first presented in [9]) are the concentrations in active drug (in the general circulation compartment, in the tumor, and in the jejunal mucosa), the population of jejunal enterocytes and the tumor cell population. The time-dependent sensitivity of both the tumor and healthy cells to the drug is taken into account by 24-hour periodic modulation of the maximum of the PD function inducing cell death. The identification of model parameters was performed as far as possible on experimental laboratory data, precisely tumor size evolution curves during active treatment, i.e., a sequence of oxaliplatin injections, versus inactive treatment, i.e., the same sequence of injections of the sole drug vehicle.

1.3. Application chosen for this feasibility study

Oxaliplatin is one of the few drugs active on human metastatic colorectal cancer [10]. It is also known to be active on Glasgow osteosarcoma (GOS) in $B6D2F_1$ mice, and the treatment of this murine tumor has been extensively studied in our laboratory (INSERM U 776 "Biological Rhythms and Cancers", Paul-Brousse Hospital, Villejuif, France) according to various time-scheduled dose regimens [11].

Fragments of Glasgow osteosarcomas, about 1 mm^3 in volume that were sampled from fresh tumors in $B6D2F_1$ mice, were inoculated by subcutaneous puncture into both flanks of animals of the same lineage. Tumor size, from the moment it had become palpable just under the skin in the tumor-bearing animals until their sacrifice on ethical grounds, was measured with a caliper by its highest and lowest diameter, three times per week. The time evolution of tumor weight, deduced from these measures by an approximation formula (proportional to $L \times l^2$, longer and shorter diameters, respectively), was the basis for assessing tumor growth and therapeutic efficacy [11]. Within four weeks, all mice were dead, by toxicity or tumor development, or they had been sacrificed on ethical grounds when the tumor grew to a weight of 2 g.

In the present study, the population of jejunal enterocytes was chosen as a healthy tissue toxicity target in mice. Leukopenia is another known target of oxaliplatin toxicity in mice, but the main damage documented after time-scheduled injections of oxaliplatin was extensive jejunal mucosa necrosis [12]. For another cytotoxic drug, the bone marrow can be used as a target of drug toxicity, possibly using the same type of model, or more likely models of a different type, e.g., involving differential equations with delays in cell cycle models as reviewed e.g. in [13].

The total dose per course in the model simulations was limited to 20 mg/kg of oxaliplatin (300 μg of free platinum for a 30 g mouse). Actual doses in laboratory experiments consisted of four daily injections of 4 mg/kg of oxaliplatin [11].

1.4. Physiological hypotheses, literature data and model assumptions

1.4.1. Pharmacokinetics

Free platinum (Pt) is the active form of the drug; it binds *irreversibly* to all DNA bases, which is the assumed main mechanism of its efficacy and toxicity [14–17]. It also binds more avidly to sulphydryl radical-containing molecules, such as reduced glutathione, that protect cells from Pt toxicity [14] and also contribute to its elimination from blood by uptake and irreversible binding in erythrocytes. In oxaliplatin, Pt is linked to a diamminocyclohexane (DACH) nucleus (which is thought to be responsible for the poor DNA mismatch repair mechanisms and hence higher activity in colorectal cancer, in comparison to cisplatin [18]), and to an oxalate ion, a compound structure which endows it with relatively good blood solubility. Diffusion through membranes is ensured thanks to a transporter protein, a mechanism thought to be linear (i.e., no saturation is seen on outward/inward concentration transfer curves), based on in vitro assessments [19].

It has been assumed in this model that DACH–Pt oxalate (oxaliplatin) diffuses freely in the plasma and is eliminated as a free molecule from the (central) plasma compartment by binding irreversibly to plasma or hepatic proteins or to erythrocyte glutathione according to first-order kinetics [14,17,20]. In the periphery, DACH–Pt is transported through cell membranes according to a linear mechanism to the healthy cells and, in parallel, to the tumor cell compartment. Also according to first-order kinetics, either it is degraded there (mainly by intracellular glutathione) or it reaches its DNA target. This knowledge led to the definition of a single central compartment for soluble Pt and two peripheral compartments for nucleic acid-bound Pt, one for the tumor and one for the healthy tissue, here the jejunal mucosa. DACH–Pt binding to plasma proteins is fast and irreversible [14,20], and its intracellular binding either to DNA or to reduced glutathione and other detoxification molecules is also supposed to be rapid and irreversible. Its binding to plasma proteins and red blood cell reduced glutathione in the central compartment, on the one hand, and to peripheral cellular reduced glutathione and other detoxification molecules, on the other hand, may thus be represented by simple elimination terms. The parameters of natural Pt elimination in the tissues may be evaluated by the evolution of total Pt tissue concentrations, assuming proportionality between nucleic acid-bound and total Pt tissue concentrations.

1.4.2. Pharmacodynamics

Drug activity is represented by an efficacy/toxicity function (Hill function) inhibiting cell population growth in each peripheral compartment, healthy tissue or tumor. This function is here supposed to depend only on tissue drug concentration and the time of drug exposure, with a time-dependent amplitude modulation, here figured by a plain cosine function, representing circadian drug sensitivity.

1.4.3. Enterocyte population

The enterocyte population is known to respond to radiologic or cytologic insult by damped oscillations converging to its initial and stable equilibrium value [21,22]. The stability of this equilibrium is ensured physiologically by exact compensation (tissue homeostasis) of the villi cells eliminated into the intestinal lumen by the influx of young cells from the crypts.

It is also assumed that only crypt cells (the renewing ones, in which cell cycle activity exists) are subject to drug toxicity.

1.4.4. Tumor cell population

Without treatment, tumor growth is assumed to follow a Gompertz law [23]: firstly exponential growth, then convergence towards a plateau. This is representative of the early stages of tumor growth, before neoangiogenesis induces regrowth. The particular choice of the Gompertz model for such an S-shaped curve may be justified by considerations of the existence of proliferative and quiescent subpopulations in the tumor [24,25]. Though more elaborate models might be used, for instance using partial differential equations for tumor growth and inhibition by drug contact [26,27], or modifications of the Gompertz model, itself, obtained by making the upper limit, B_{max}, dependent on time so as to take angiogenesis into account [28,29], we chose to represent the first stages of tumor growth only, and to assess optimization procedures on such a

basic model endowed with but few parameters. Drug resistance may also optionally be introduced into the model as the probability for a given tumor cell to develop such resistance [30], though this is not considered here.

2. The model

2.1. Pharmacokinetics

The three dynamic variables considered here are Pt concentration (oxaliplatin being a compound DACH–Pt oxalate) in the central, or plasma, compartment, P, and nucleic acid-bound Pt concentrations in the healthy tissue (jejunal mucosa), C, and in the tumor, D. The first-order kinetic equations are:

$$\frac{dP}{dt} = -\lambda P + \frac{i(t)}{V_{di}} \tag{1}$$

$$\frac{dC}{dt} = -\mu C + \xi_C P \tag{2}$$

$$\frac{dD}{dt} = -\nu D + \xi_D P. \tag{3}$$

Here λ, μ and ν are decay parameters representing Pt elimination by *irreversible binding* to plasma proteins, hepatic or red blood cell glutathione, on the one hand (λ), and to intracellular glutathione or protective proteins, on the other hand (μ for healthy cells and ν for tumor cells). Parameter V_{di} is the drug distribution volume, which is assumed to be constant, in the central compartment, and i: $t \mapsto i(t)$ is the drug infusion flow control law. The flow i may be a constant function, in the case of constant continuous infusion, or a periodic one, in the case of a time-scheduled drug regimen, as is commonly used in clinical settings, and in the latter case may show different forms: square, sinusoid-like, or sawtooth-like waves, all of which are clinically implemented using programmable and portable infusion pumps like the ones that have been used for delivering the chronotherapy of cancer medications over the past several years; it may also be a brief, quasi-dirac-like impulsion function in the case of bolus administration, or any continuous function of time. Factors ξ_C and ξ_D before P in the second and third equations represent active drug transfer rates from the plasma to the peripheral compartments.

2.2. Pharmacodynamics: toxicity and therapeutic efficacy functions

These functions represent the mean drug activity in the healthy and tumor cell populations considered here, and are functions of the drug concentration, in the healthy tissue for toxicity, and in the tumor tissue for therapeutic efficacy. Both are Hill functions, modulated in amplitude by a circadian chronosensitivity factor:

$$f(C) = F \cdot \left\{1 + \cos\left(2\pi \frac{t-\varphi_S}{\mathcal{T}}\right)\right\} \cdot \frac{C^{\gamma_S}}{C_{S50}^{\gamma_S} + C^{\gamma_S}}$$

$$g(D) = H \cdot \left\{1 + \cos\left(2\pi \frac{t-\varphi_T}{\mathcal{T}}\right)\right\} \cdot \frac{D^{\gamma_T}}{D_{T50}^{\gamma_S} + D^{\gamma_T}}$$

where C and D are as defined earlier, γ_S and γ_T the Hill coefficients (>1 if drug activity is known to show cooperative reaction behavior as in certain enzymatic reactions, and by default equal to 1 if drug binding to its target, and subsequent cell death, is assumed, as will be the case here, to follow Michaelis–Menten kinetics), C_{S50} and D_{T50} half-maximum activity concentrations, F and H the half-maximum activities, $\mathcal{T}=24$ h (period of circadian drug sensitivity oscillations), and φ_S and φ_T are phases (in hours with reference to a fundamental 24-hour rhythm, i.e., taking into account 24-hour periodicity) of the maximum activities of functions f and g.

2.3. Enterocyte population

Growth of the enterocyte population evolution in an arbitrarily fixed volume of jejunal mucosa is represented by two dynamic variables: the mature villi cell population, A (in number of cells), and the flow, Z (in number of cells per time unit), of incoming young cells counted positively which migrate per each time unit from the crypts to replace ageing villi enterocytes that are eliminated into the intestinal lumen (Fig. 1):

$$\frac{dA}{dt} = Z - Z_{eq} \tag{4}$$

$$\frac{dZ}{dt} = \{-\alpha - f(C)\}Z - \beta A + \gamma. \tag{5}$$

Here $f(C)$ is the drug toxicity function in the healthy tissue introduced earlier, α a natural autoregulation factor in the crypt which the drug toxicity function thus modulates additively, β a mitosis inhibitory factor (a so-called "chalone") supposedly sent from the villi to the crypts, Z_{eq} the steady state (constant) flow from crypts to villi, and $A_{eq} = \frac{\gamma - \alpha Z_{eq}}{\beta}$ the steady the steady state villi population (without treatment). In healthy jejunal mucosa, tissue homeostasis (here represented, in the absence of drug damage, by constant cell population at steady state) is granted, so the equilibrium point (Z_{eq},A_{eq}) is a stable one. The parameters of the damped harmonic oscillator (Z,A) are entirely determined

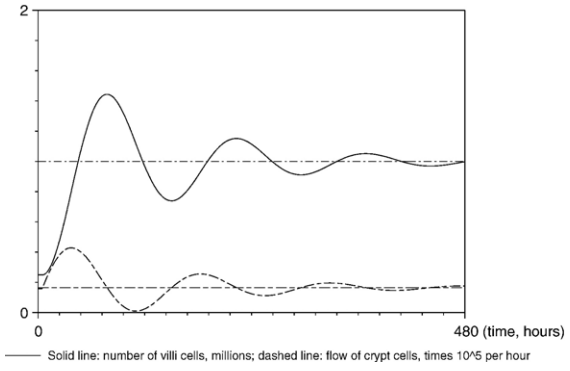

Fig. 1. Model oscillations of the population of enterocytes in response to a brief radiotoxic or cytotoxic insult shown over 20 days. Villi cells (top) and flow from crypts (bottom) are represented here recovering in a steady state behavior after an initial deviation from their equilibria at time zero. They may be seen as the linear approximation of a more complex phenomenon, e.g., as proposed in [31]. Units are in millions of cells for villi (solid line) and in units of 10^5 cells for the flow of cells from crypts (dashed line). Time (abscissa) is in hours.

if its period and dampening coefficient, together with the equilibrium point coordinates, are known (they can indeed be determined by elementary computation, as shown in the Appendix).

2.4. Tumor growth

Tumor growth is represented by the number of tumor cells, B, which is assumed to follow the Gompertz law without treatment, modified by a "therapeutic efficacy term" $-g(D)\cdot B$:

$$\frac{dB}{dt} = -a\cdot B\cdot \ln\left(B/B_{\max}\right) - g(D)\cdot B \qquad (6)$$

where $g(D)$ is the therapeutic efficacy function earlier introduced (here seen as a instantaneous death rate in the tumor cell population), $B_{\max}$ is the asymptotic (that is, maximal, since without $\frac{dB}{dt}>0$) treatment value of B, a is the Gompertz exponent, i.e., without treatment, one has $\frac{dB}{dt} = G.e^{-a(t-t_0)}\cdot B$, where $G = \frac{1}{B(t_0)}\frac{dB}{dt}|_{t=t_0}$ is the initial growth exponent if t_0 is the chosen initial observation time, conveniently estimated on the initial part of a tumor growth curve without treatment. Without treatment, this integrates immediately in $B(t) = B(t_0)e^{\frac{G}{a}\left(1-e^{-a(t-t_0)}\right)}$, whence $B_{\max} = B(t_0).e^{G/a}$. An example is shown in Fig. 2.

3. Model identification and computer simulation

3.1. Drug doses and pharmacokinetics

In the case of constant or periodic delivery regimens, the daily dose of active infused drug (Pt in oxaliplatin) was fixed as 60 μg of free Pt (corresponding to 4 mg/kg/d of oxaliplatin for a 30 g mouse, a common dosage for the laboratory, where the daily doses range between 4 and 17 mg/kg). Diffusion parameters (V_{di}=10 mL, λ=6, μ=0.015, ν=0.03) were estimated according to published laboratory data [20] on plasma concentration and half-life of free Pt in plasma and total Pt in peripheral tissues (jejunal mucosa for toxicity and red blood cells for therapeutic efficacy, in the absence of actual data on tumor tissue); the value $\nu=2\mu$ corresponds to the elimination of the total Pt from the tumor being twice as fast as in the healthy jejunum.

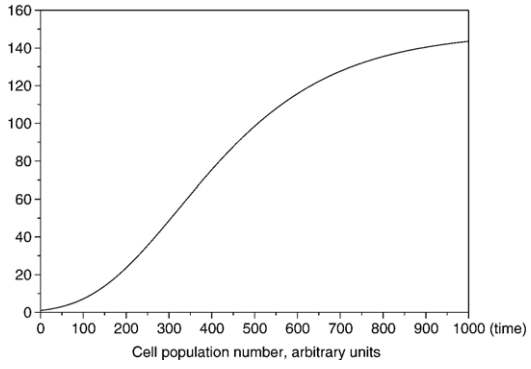

Fig. 2. Example of simple model Gompertzian growth: $B(t)=B_0e^{G/a(1-e^{-at})}$ where, $G/a = \ln\frac{B_{\max}}{B_0}$, a=0.005 and $B_{\max}/B_0$=150; time (x-axis) and number of cells are here in arbitrary units, from a minimum value B_0 arbitrarily set to 1 on the y-axis to a maximum value $B_{\max}$.

3.2. Pharmacodynamics

Hill exponents γ_S and γ_T were arbitrarily fixed as 1 in the absence of data on the actual concentration efficacy dependence, and C_{S50} and D_{T50} were set to a high value (10) compared to the average drug tissue concentrations in the model, so as to bring the efficacy/toxicity functions into a linear zone, in the absence of data on these Hill, or Michaelis–Menten functions at the tissue level.

The optimal injection phase (i.e., circadian time) of an oxaliplatin bolus was identified from laboratory experiments as 15 h after light onset (HALO), which corresponds to the middle of the activity time in the nocturnally active mice housed under a 12 h light–12 h dark regimen. This dosing time was observed to be optimal in both senses simultaneously: optimal in the sense that it yielded best anti-tumor efficacy and also optimal in the sense that it led to least drug-induced toxicity. This remarkable experimental result — a coincidence that has been always observed in experiments with mice in our laboratory, with no explanation so far, was obtained with a time resolution of 4 h by recording survival and tumor weight evolution in six different groups of mice, each group being defined by a specific HALO designation corresponding to the circadian time at which the animals received bolus injection of oxaliplatin for four consecutive days (see [11] for details). The maximal anti-tumor efficacy phase (φ_T=21 HALO) for a bolus was deduced by numerical variation along a one-hour step grid in simulations of the model. This delay $\Delta\varphi$ of approximately 6 h (from 15 HALO to 21 HALO) between the optimal injection phase φ_I – note that for a bolus the peak phase and the phase of the beginning of infusion, φ_I, coincide – and the maximal efficacy phase φ_T in the model may also be obtained by direct computation (see the Appendix). The maximal healthy tissue toxicity phase was estimated as φ_S =9 HALO based on two convergent considerations. First, we assumed by our cosine model of chronosensitivity a 12 h delay between highest and lowest drug-induced toxicity phases – and we already knew the circadian phase of lowest toxicity – and second, the circadian phase φ_S=9 is also known to be the phase of the minimum concentration of non-protein sulphydryl compounds (i.e., reduced glutathione and cysteine, the main actors in the tissue detoxification of oxaliplatin) in mouse jejunum cells [32].

In the absence of data on the evolution of jejunal cell population under treatment, the parameter F was adjusted (F=0.5) so as to yield a residual villi population always greater than 10% of the initial cell population for daily doses lower than 200 μg of free Pt (the approximate lethal dose effect for a 30 g mouse). The parameter H was estimated from tumor size evolution curves derived from animals under treatment (see Fig. 2) to obtain a likely value which was then fixed; the value then used in further simulations was H=2 (see the Appendix for details).

3.3. Healthy and tumor cell proliferation

The equilibrium point (Z_{eq},A_{eq}) for the enterocyte model was $(16{,}500,10^6)$, the latter value arbitrarily fixed and the former proportionally fixed according to data previously published in the literature [21]. The period of oscillations (6 days) and dampening coefficient (1/3) were also estimated using data found in the literature [21,31], whence α, β, γ (see Appendix for details). The initial growth exponent G and the Gompertz exponent a, whence $B_{max}/B(t_0)=e^{G/a}$, were first estimated based upon tumor size evolution curves (see Fig. 3) without treatment. Their values varied from one individual to the other (a between 0.005 and 0.1, B_{max} between 1.2 and 30 times the value of B at the beginning of its steep increase). Intermediate values chosen were $a=0.015$ and $G=0.025$, leading for the parameter B_{max} to a value of 5.3 times the initial observed value $B(t_0)$ at the onset of steep tumor growth. These values were retained so that further simulations might correspond to a human-like situation where the tumor grows rapidly, in a bounding environment, and being the object of an efficient chemotherapy (see Appendix for computational details).

The attainable parameters for model identification in clinical settings should thus be a and B_{max} for natural tumor growth, and H for therapeutic response.

3.4. Computer simulation

Numerical integration of the system of six ordinary differential equations was performed first in SCILAB or in MATLAB, then using programs written in fortran. The time unit was the hour, counted from 0 HALO on day 1. Integration (observation step: 0.1 h) began with treatment; the applied solvers were Adams and an implicit (BDF) scheme. The set of initial values was $(P_0=0,\ C_0=0,\ D_0=0,\ A_0=A_{eq}=10^6,\ Z_0=Z_{eq}=16{,}500,\ B_0=10^6)$. In clinical-like conditions that mimic hospital settings in where medications are delivered on a 24-hour basis, the chosen periodic control law was either a square, a sawtooth-like, or a sine wave.

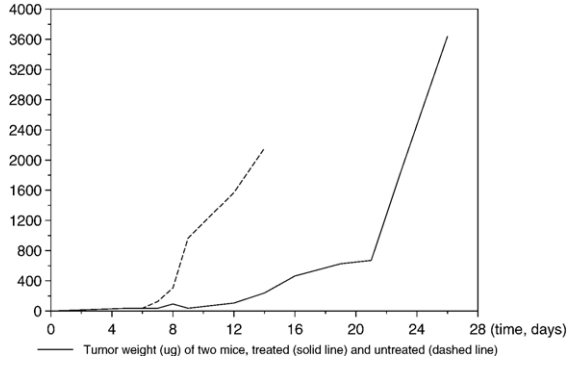

Fig. 3. Examples of tumor growth curves: without treatment (dashes) and after four evenly spaced injections (on days 5, 6, 7 and 8 following tumor inoculation into the test animals) of oxaliplatin, 4 mg/kg (solid line) in two $B6D2F_1$ mice bearing a Glasgow osteosarcoma. When tumor weight grew to two grams, animals were sacrificed on ethical grounds. Tumor weight is in units of mg (y-axis) and time is in units of days (x-axis).

4. Results: optimizing cancer chronotherapeutics

4.1. Frames for therapeutic optimization

In a first attempt, we adopted the types of drug-delivery regimens which are common in clinical therapeutics. Usually they entail infusion times of 1 to 12 h each day, periodically repeated on a 24-hour basis over four or five days, followed by a drug-free interval of time to allow patient recovery from drug-induced toxicity. This course of treatment is repeated every other week (when the duration of effective treatment is four days per course) or every third week (when the duration of effective treatment is five days per course). The optimal peak infusion time being known from previous experimental data, the search for optimality then consisted of obtaining the best infusion duration for the best daily regimen chosen among a limited dictionary of infusion profiles, of square, triangle, or sine wave shape. This best infusion was determined by varying this duration from 1 to 12 h by one-hour steps for each profile, and evaluating the resulting number of residual tumor cells.

Then we decided, using mathematical optimization techniques, to remove the periodical infusion scheme constraint, still taking into account the optimality of the peak infusion times, which is represented in the model by a sinusoidal modulation of the maximum effect. This yielded other optimal therapeutic drug-delivery schemes.

These two different attitudes toward therapeutic optimization and their results are described below.

4.2. Mimicking hospital routines: 24-hour periodic chemotherapy courses

A typical five day-infusion chemotherapy course, with the first five days of recovery, is represented in Fig. 4, where one can see the six variables of the dynamic system, from top to bottom: P, C, Z, A, D, and $\log_{10}(B)$. The objective function (to be minimized) is the minimal number of tumor cells (ideally zero) and tolerability consists of preserving a minimal number of villi cells, a percentage of the arbitrary initial value of 10^6 cells.

A graphic illustration of injection phase optimization in the model is presented in Fig. 5. The plateaus (centered on maximum anti-tumor efficacy phase φ_T) represent the logical variable $L=\left(a\ln\frac{B_{max}}{B}-g(D)<0\right)$ that is highly dependent on drug chronosensitivity in the tumor: 1 when the drug actually inhibits tumor growth, 0 when it does not. The optimization principle used here (numerically varying the circadian phase φ_I of the beginning time of infusion) may be seen as graphically superimposing the areas under peaks of tumor drug concentration (D, sawtooth line) on these plateaus ($L=1$). Tumor cell population evolution is shown in parallel on a logarithmic scale.

Therapeutic optimization may take place in two different contexts, depending on the patients' state of health, based on clinical criteria (to be evaluated by physicians), leading to two different schemes: either an aggressive curative scheme for patients who are able to tolerate a high degree of toxicity in the hope of obtaining complete tumor eradication, which is the

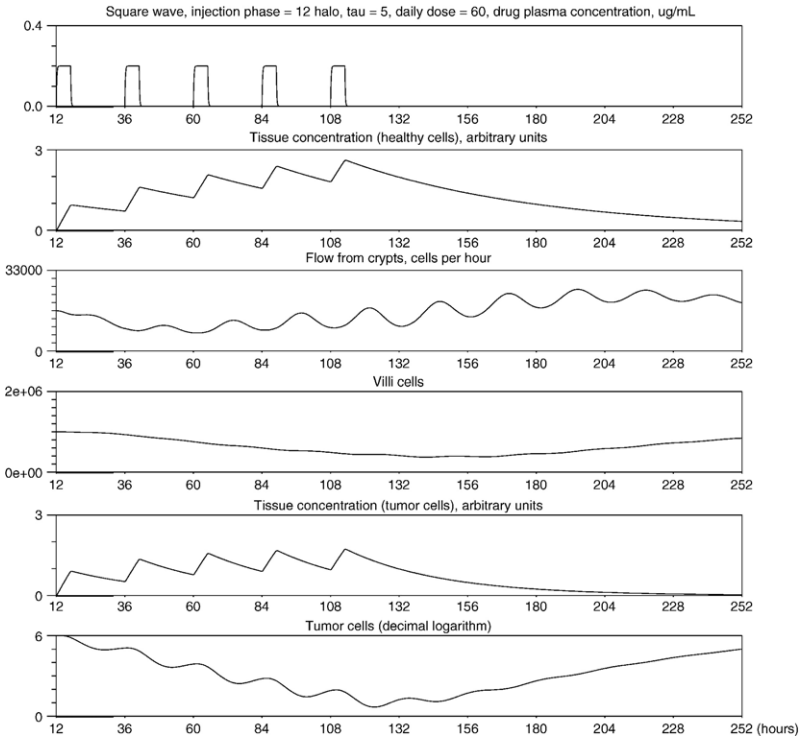

Fig. 4. A five-day optimal time-scheduled 24-hour periodic regimen followed by five days of recovery. Time (abscissa) is in hours and quantities in ordinates in units that depend on the track considered: μg/mL for drug plasma concentration, arbitrary units for tissue drug concentrations (depending on an unknown transfer constant from plasma to tissue) and cell populations in number of cells.

main goal of therapy; or a reduced toxicity scheme, leading only to tumor stabilization, i.e., forsaking eradication but maintaining an absolute limit of healthy cell toxicity, within which one is left with as few tumor cells as possible at the beginning of recovery time (usually followed by repeated subsequent courses of chemotherapy in order to contain the tumor). Transposed in the context of this model study, this choice between an aggressive and a reduced toxicity scheme led to the definition of two different types of simulations.

4.2.1. Simulations focusing on anti-tumor efficacy

The criterion for the "aggressive curative scheme" was to yield the smallest number of tumor cells during the course of chemotherapy (5 days of treatment and 16 days of recovery) for a standard daily dose of 60 μg/d of free platinum. A possible temporary decrease in the mature enterocyte population to as low as 35% of the initial population was allowed (compare this threshold with the previous one of 60% in the reduced toxicity scheme; these values are arbitrary in the absence of data known to us on the severity of diarrhea related to mucosal depletion, but they could easily be changed).

For the square wave control law, the best result (four residual tumor cells out of 10^6 initially) was obtained with an effective five-hour infusion duration that begins at 12 HALO. Even a better result (3 residual tumor cells) than with this five-hour square wave for the same daily dose was obtained with a sharp sinusoid-like model infusion law lasting five hours that begins at 12 HALO. Respect for the optimal injection phase is essential, since constant infusion yields worse results (16 cells) than square wave time-schedule beginning at optimal injection phase $\varphi_I = 12$ HALO (four cells), but achieves better results than the beginning time coinciding with the worst phase of 0 HALO (52 cells). In other words, this means that chronotherapy can be worse than constant infusion if the beginning infusion time φ_I is ill-chosen.

These simulations show in this theoretical framework the advantages of a time-scheduled regimen as compared to the conventional constant infusion scheme, *provided that the beginning infusion (circadian) time φ_I is accurately chosen*. Note that this last point is dependent on the chosen drug, not on the individual, inasmuch as the fundamental circadian rhythms

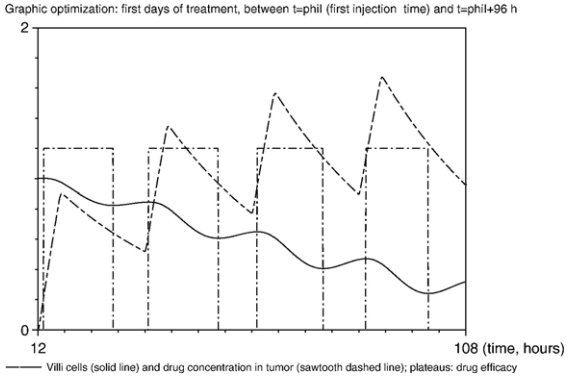

Fig. 5. Graphic chronotherapeutic optimization. Solid line = tumor population, logarithmic scale $\log_{10}(B)$; dashed line plateaus: up when the drug actually inhibits tumor growth, down when it does not; sawtooth dashed line = drug concentration in the tumor shown in arbitrary units; time shown in hours.

of the individuals in a population (as determined by their body circadian clocks [33]) are synchronized by environmental time signals of light, meals, social life, etc.; this was the case for the nocturnally active mice of this study that were all previously synchronized to a regimen of 12 h light alternating with 12 h darkness. These simulations also suggest that sinus-like waves actually used in clinical chronotherapies are a good approximation for optimality in this context.

4.2.2. Simulations focusing on treatment tolerability

The criterion for the reduced toxicity scheme was prohibition of the decrease of the mature enterocyte population below a given threshold (arbitrarily fixed between 40% and 60% of the initial population value) to obtain the therapeutic regimen yielding, by variation of the drug daily dose, the smallest number of tumor cells during the course of chemotherapy (in this case, 5 days of treatment and 16 days of recovery).

In the case of the threshold to preserve 60% of the initial population of enterocytes, the best result (2400 residual tumor cells out of 10^6 initially) was obtained with a right sawtooth-like infusion model law lasting 2 h (i.e., steep increase, then drop) beginning at $\varphi_I = 14$ HALO, allowing the infusion of a maximum dose of 33 µg/d of Pt. In the perspective of applications to clinical settings, the main drawback of this time schedule is the achievement of very high drug concentrations over a short period of time; in humans, at least a two-hour duration of oxaliplatin infusion is recommended to prevent acute muscular toxicity, in particular laryngeal spasm, an acute

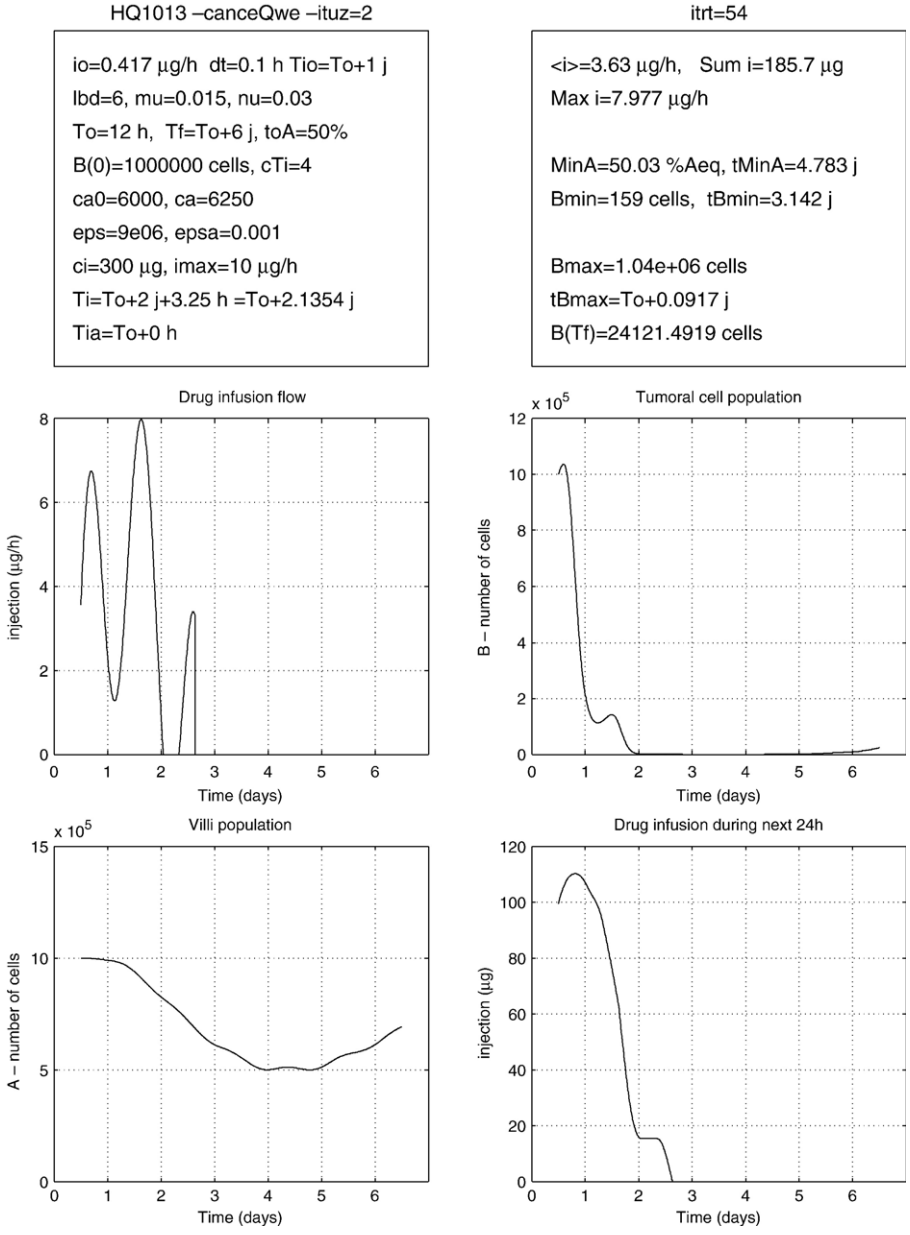

Fig. 6. Optimal eradication treatment preserving at least 50% of jejunal enterocytes: instantaneous drug infusion flow i (in µg/h), tumor cell population *B*, villi cell population *A*, and the resulting dose (in µg) – obtained by integration of *i* between times *t* and *t*+24 h – administered over a sliding window of 24-hour duration. Figure courtesy of C. Basdevant. See Ref. [38] for further details.

toxicity symptom which imposes termination of treatment. Such acute toxicity is excluded in the model, where chronic jejunal toxicity is the focus, by setting an upper limit to the drug infusion flow and its derivative with respect to time. The advantage of this reduced toxicity scheme is better anti-tumor outcome compared to the conventional constant infusion therapy that, for the same limit toxicity, imposes (in the model) a dose delivery no greater than 29 μg/d of Pt (7000 residual tumor cells).

These simulations illustrate in a modeling frame what is well known to oncologists involved in chronotherapeutics: first, a well chosen time-scheduled regimen can yield better results than a constant infusion scheme, and second, the shorter the infusion time, the less intolerance to treatment, as far as *chronic* toxicity is concerned.

4.3. Drug flow optimization in a general non-periodic frame

With the same model, but removing usual clinical chronotherapeutic requirements which impose 24-hour periodicity of the infusion scheme, we set the mathematical problem of therapeutic optimization as maximizing tumor cell death under

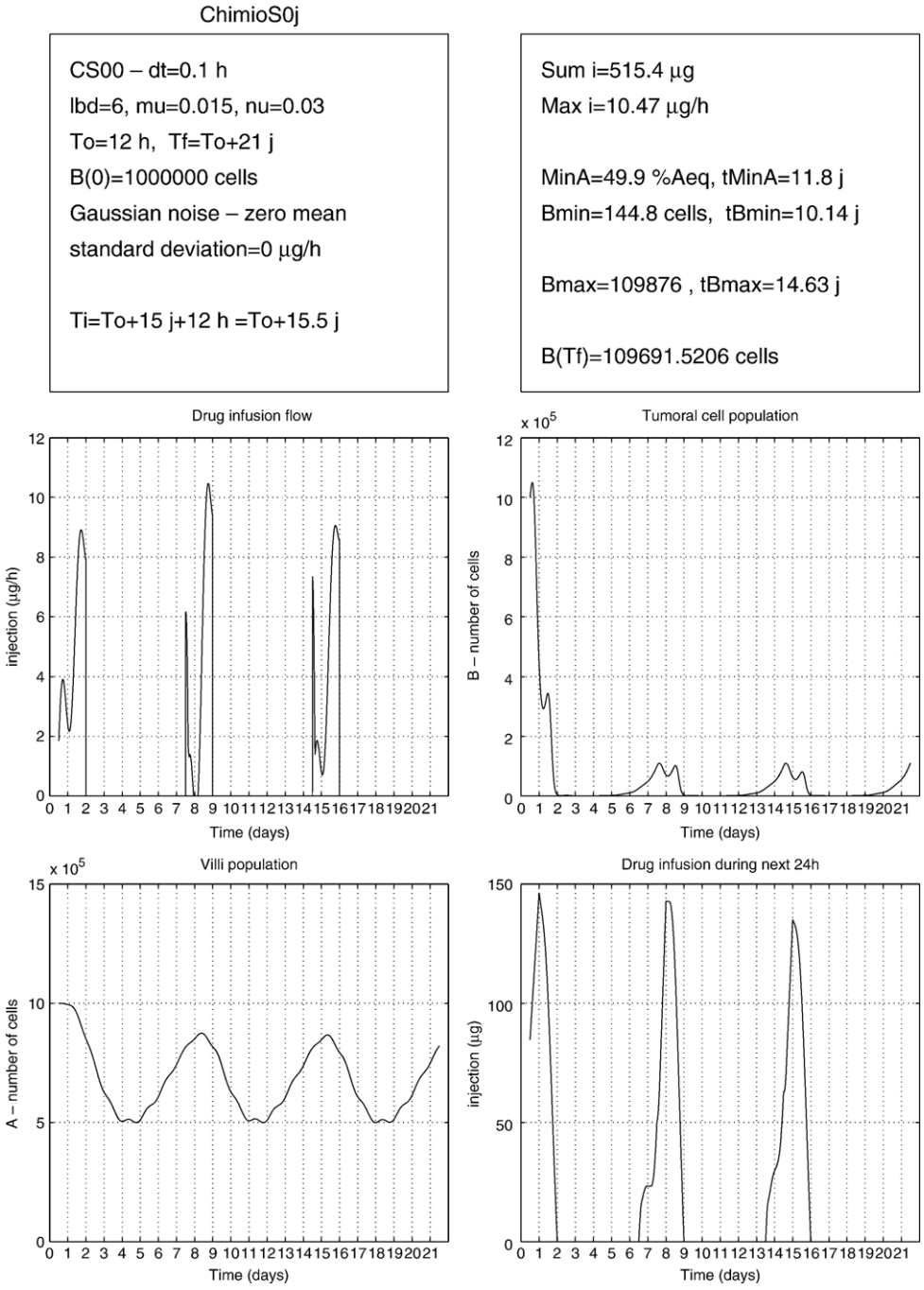

Fig. 7. Three weeks stabilization treatment with repeated chemotherapy courses of 1.5 of active medication 5.5 days medication-free interval: same variables as on Fig. 6. Figure courtesy of C. Basdevant. See Ref. [38] for further details.

the constraint of maintaining the healthy cell population always above a given threshold. This point of view has also been developed by other authors with different methods, in a similar context but with preservation of a different healthy cell population [36,37].

Whereas the clinical tolerability constraint is unequivocal (yet tunable by physicians according to the patient's state of health), the tumoral cell death maximizing goal may be understood in two different ways, since a tumor that has not been eradicated starts to regrow at the end of treatment. Either one assumes that complete eradication is possible and then the objective function to be minimized is the *minimum* number of tumor cells, as close as possible to zero, during a one course treatment; or one admits that there always will remain an ineradicable fraction of tumor cells, which may only be contained by repeated treatment courses under an acceptable threshold, compatible with patient survival. Then the objective function to be minimized is the *maximum* number of tumor cells during repeated treatment courses, in fact during the recovery period of the course.

This distinction leads to two different optimization strategies, respectively: the eradication strategy in a single course, and the stabilization strategy for repeated courses of the same treatment, which aims only at containing the tumor. This point of view has been extensively developed in a recent article, to which we refer for detailed results [38]. To briefly state the results obtained for each one of these two strategies, an optimal drug infusion flow (to be implemented using a programmable pump) is derived to minimize the tumor cell number (minimum or maximum) and to satisfy the conditions: a) the healthy cell population number remains above a given threshold; b) the total drug dose is lower than a prescribed level; and c) its instantaneous flow and its derivative with respect to time also remain below a prescribed level. Examples of these results are illustrated in Figs. 6 and 7. Since the resulting optimized infusion flows are not superimposable onto the 24-hour periodic sine wave like flows used in clinics, this suggests that classical repeated sine wave chronotherapeutic regimens are only approximations to optimality and may be further improved. Yet, in the absence of precise knowledge of all the parameters of the model, and their related confidence intervals, it would be hazardous to quantify in terms of tumor cell kill the gain expected from this optimized procedure as compared to the classical chronotherapeutic regimens.

5. Discussion and clinical perspectives

5.1. Advantages and limits of the model

The described model provides a semi-quantitative prediction tool. First, it shows that time-scheduled regimens are likely to yield a better treatment outcome than a constant infusion regimen, provided that the beginning time (with reference to circadian rhythms) φ_I of the infusion is well chosen. Second, it allows one to optimize time-scheduled regimens by acting on the beginning (or peak time) and duration of the infusion, and on the shape of the programmable infusion control law. To our knowledge, this is the first time that such clinical know-how has been set upon theoretical grounds.

The model was chosen to be a simple one to help parameter identification under the restraint of a relative scarcity of available data on the internal mechanisms of tumor growth and inhibition by medications. Its quasi-linear form without treatment (set $W=\ln B$ in the last equation and the model without treatment becomes completely linear) may be seen as a robust and natural approximation, in a neighborhood of its initial values, of a hypothetic, more complete and realistic model for cell proliferation. Some of its components, such as drug activity functions, remain unknown and were chosen according to the experience of pharmacologists working with different medications, such as antibiotics; in the same way, some parameters had to be estimated on questionable grounds, such as extrapolation from one tissue to another. Nonetheless, the other parameters were identified after experiments done in our laboratory on the effects of oxaliplatin treatment on GOS tumor-bearing $B6D2F_1$ mice.

5.2. Model assumptions

5.2.1. Healthy cell population

The linear system representing jejunal mucosa homeostasis may be seen as the linearization of an unknown non-linear system, which should describe the enterocyte population kinetics in a more accurate way (as in [31]), around its stable equilibrium point (Z_{eq},A_{eq}). Tissue homeostasis may be observed after brief radiologic or cytotoxic insult. In the case of a sudden perturbation, return to equilibrium with damped oscillations has been reported [22]. To guarantee the validity of this linear approximation, we make the additional assumption that this equilibrium point is hyperbolic, i.e., the linear tangent system has no zero or purely imaginary eigenvalues. Then linearization is valid, up to topological equivalence, in the vicinity of the equilibrium point, according to the Hartman–Grobman theorem (see for instance Perko [34]).

No basal (without treatment) circadian variation of the enterocyte population has been taken here into account; whereas, at least circadian variations in the enterocyte cell cycle have been known for some time [22,35]. The reason for this is the irrelevance of such variations for the follow up of the enterocyte population during a course of chemotherapy. The variables (Z,A) should rather be seen as sliding averages over the last 24 h of the population described beforehand. It is quite likely that instead of a basal equilibrium point, the non-linear system presents rather a stable limit cycle, with 24-hour period, but we are interested here only in controlling drug toxicity on an average villi population, since circadian variations of this population are negligible compared to the havoc produced by the drug-induced cytotoxicity.

Other toxicities such as neurotoxicity and hematotoxicity, known to be induced by oxaliplatin in human beings, were taken into account by imposing course scheduling designed as short treatment durations followed by sufficiently long recovery times, e.g., two days of treatment followed by five days of recovery in the case of repeated chemotherapy courses. Such a

recovery duration may seem short, but GOS is a fast growing tumor, with an apparent doubling time in exponential models being about 1.4 days; so, the long recovery times as used in clinical settings for curable human tumors (e.g., 10 days in 2 weeks or 16 days in 3 weeks) are not realistic here, since they would enable the tumor too much time for regrowth beyond its initial value after the end of the last infusion.

Neuropathy could not be experimentally examined in mice. Hematotoxicity (mainly leukopenia) was assumed in this study to be made up for by natural bone marrow proliferation during recovery. Post-mortem histology performed in animal experiments in our laboratory showed tolerable bone marrow depletion; in contrast, jejunal toxicity was most severe, with extensive necrosis of the mucosa [12,20].

5.2.2. Tumor cell population

The initial value for the tumor cell population number was arbitrarily fixed as 10^6 cells, and eradication was considered complete when it became lower than 1. These values could easily be replaced by 5×10^9 and 200 (oncologists agree on these figures, which represent a frequent lower limit for clinical or radiological discovery and a cell population number under which a tumor is usually considered as non-viable). The optimality, in the conditions of our model, of the infusion duration and initial phase (between 0 and 24, i.e., taking into account 24-hour periodicity) will not be changed by such modifications, given the homogeneity of Eq. (6) and the scale independence of the chosen criterion $\left(\min_{t\in[0,T]} B(t) \text{ or } \max_{t\in[0,T]} B(t)\right)$.

It is possible to introduce drug resistance in tumor cells, following Goldie and Coldman [30], by replacing in Eq. (6) the cell kill term $-g(D).B$ by $-g(D).B.\frac{1+B^q}{2}$ where q is -2 times the probability for a cell to become resistant, a probability that in this formulation is independent of the time of or the amount of delivered dose, yielding a population of $B.\frac{1-B^q}{2}$ resistant cells; for instance, if one out of a thousand cells acquires drug resistance, then $q=-0.002$.

5.2.3. Pharmacodynamics

No cell cycle phase specificity of oxaliplatin has been reported, which is consistent with its supposed mechanism of action at the cell level, i.e., binding to DNA at any stage of the cell cycle. This makes inclusion of cell cycle kinetics in the present model unnecessary, at least as long as oxaliplatin is the only cytotoxic drug used for pharmacological control and circadian drug sensitivity is represented in the above-mentioned simplified way.

Drug toxicity and anti-tumor efficacy functions have been chosen to act as multiplicative factors on the population size of enterocytes and tumor cells. While this assumption is quite natural in the linear frame of the enterocyte model, where $f(C)$ is just an enhancement of the natural autoregulation coefficient α, it is more questionable for the Gompertz tumor growth model: it has the consequence "big tumor, big effect; small tumor, small effect". This may be true for oxaliplatin, but not for other drugs; other representations of the anti-tumor effect could be used instead of $-g(D)B$, such as $-g(D)\frac{B}{K+B}$, as in [26].

The only place in the model where circadian variability occurs is by modulation of the maximal drug effect (parameters F and H). This simplifying assumption thus aggregates all possible circadian influences on one term in each peripheral compartment. The actual physiological circadian variation in drug sensitivity is more likely due to the variations in drug detoxification mechanisms in the central (hepatic enzymes, plasma proteins) and peripheral (cellular glutathione) compartments, but tissue measures which would be necessary to identify the parameters of these chronopharmacokinetic (i.e., biological rhythms in drug pharmacokinetics) mechanisms were not available to us, even though one may hope they will become available through future routine laboratory experiments or clinical data investigations.

The representation of drug chronosensitivity by a plain cosine intervening as a multiplying factor in the expression of the drug activity functions may be considered to be a coarse description of circadian rhythmicity. In the same way, this model does not include recent advances in the knowledge of the genetic determinants of mammalian circadian rhythms, such as the clock genes CLOCK, BMAL1, PER and CRY (and their proteins), nor of their influences on the cell cycle of the cellular populations involved [5–7]. In this respect, the cosine model might be replaced by a circadian oscillator model of the type developed by A. Goldbeter for *Drosophila* [2] or for mammals [3,4] or even by a simple Van der Pol oscillator, as suggested in [39]. But, as it is, this cosine function takes pragmatically into account the chronomodulation of the PD by circadian factors which has been observed in experimental and clinical settings.

5.3. Possible extensions of the model

5.3.1. Perspectives for clinical applicability

The design of this model originated from the desire to improve already existing time-scheduled regimens used in chronotherapeutics, mainly for metastatic colorectal cancer. But the present identification of its parameters in a population of mice, especially those related to untreated tumor progression, is not easily transposable to the clinic for evident ethical reasons. Yet if we want to apply chronotherapeutic optimization procedures outlined in this paper in clinical settings, we need to evaluate for a given cancer in a given patient the parameters of tumor growth dynamics and of drug response.

In particular, in order to give confidence intervals for the results of therapeutics optimized with the help of this model, a linear sensitivity analysis of the space of its parameters clearly remains to be done, and this will be accomplished in a future and extended version of this work. Nonetheless, individual patient tailoring of therapeutics involves developing for this model *population PK and PD* parameter evaluation methods which will require a better understanding of the various forms of tumor growth, relying on mathematical modeling and the analysis of in vitro, experimental and clinical data.

This presented model is thus intended to serve as an introductory example to the use of a general method for therapeutic optimization. Further modeling work is yet required to take

into account the accumulating knowledge of tumor growth dynamics and to apply this model in the everyday treatment of cancer patients, which uses combinations of different cytotoxic drugs.

5.3.2. Toxicities

Other toxicities need to be considered. In the perspective of future applications to medicine, it must be stated that oxaliplatin toxicity in human beings consists of peripheral sensory neuropathy, diarrhea and vomiting (taken here into account by jejunal toxicity), and hematological suppression [14].

Neurotoxicity is usually reversible in humans. As mentioned earlier, when it does not manifest itself as an acute symptom, such as laryngeal spasm which imposes immediate cessation of the treatment (this is normally avoided by averting high instantaneous drug concentration flows). it is a chronic toxicity, dependent on the total delivered dose, which imposes in clinical settings only a minimum recovery time between courses of chemotherapy. The prevention of acute neuropathy is taken into account in the model by imposing an upper limit to the drug infusion flow and its first derivative with respect to time.

In the perspective of clinical applications, hematotoxicity is not an issue in colorectal cancer *chronotherapeutics* by oxaliplatin and 5FU; whereas, intestinal toxicity is. For instance, it has been shown that in a pilot clinical trial [40] of oxaliplatin and 5-Fluorouracil (5FU) in patients with colorectal cancer, comparing chronotherapeutic time-scheduled regimen with the more widely used FOLFOX2 protocol, fewer episodes of neutropenia and more numerous episodes of diarrhea occurred in the chronotherapy arm.

It is clear that the future inclusion of other cytotoxic drugs in model therapeutics will imply considering the representation in the model of other such toxicities.

5.3.3. Molecular pharmacology modeling to explain drug synergies

Some future extensions of this model will be necessary to actually help oncologists, such as representation of several drugs acting in the same chemotherapy course (for instance oxaliplatin, 5FU and folinic acid, as currently used in combination for the treatment of human colorectal cancer). To account for synergies between drugs and their optimization, as much as possible such PD modeling should be led at the molecular level within a model of the cell cycle. For instance, oxaliplatin action should be represented by the damage it exerts directly on DNA as a function of its intracellular concentration; whereas, the PD of 5FU should be represented by its action on thymidylate synthase during the S phase of the cell cycle. The resulting cell kill in fast renewing tissues will then be due to phase transition blocking and apoptosis induction, in particular, by the protein p53. Models which partly take into account cell cycle dynamics of tumor growth and therapy already exist [41–43], but considerable work remains to be done to represent multidrug-induced modifications at the molecular level in a model that will be useable by oncologists in the clinic.

5.3.4. Drug resistance and other problems not considered here

Other options include representation of a tumor drug resistant cell population as an independent dynamic variable, as in [44,45] with possible dependence of the probability of transition to resistance on the drug dose level, genetic polymorphism in the response to cytotoxic drugs (this may be done more easily in molecular PK–PD models), and all other issues linked to metabolic and tissue environmental factors such as tumor angiogenesis, local and remote invasion, some of which are representable by reaction–diffusion equations for tumor growth and therapy, as in [26,27]. These manifestations of cancer growth may also be included as targets for anticancer therapy, i.e., included in an objective function to be optimized; whereas, emerging resistance linked to high drug doses provides a supplementary constraint comparable to clinical tolerability in healthy tissues. These complementary problems can thus be taken into account as objective functions and constraints for optimization methods in extended versions of the model without changing the principle of balancing therapeutic efficacy and unwanted adverse medication effects.

Acknowledgments

I am gratefully indebted to Michael Smolensky who did not spare his time in helping to revise the manuscript.

Appendix A. Parameter identification procedures

A.1. Enterocyte model

As mentioned in the text, tissue homeostasis (conservation of the cell population number, at least in the mean, i.e., averaged over 24 h and thus independent of circadian factors) of the jejunal mucosa may be represented by an equilibrium point of a dynamic system. Since convergence towards equilibrium is experimentally obtained with damped oscillations, the model should be of dimension 2 at least, but dimension 2 is also sufficient to design a linear oscillating model. Besides, assuming hyperbolicity of the equilibrium point, the Hartman–Grobman theorem allows us to replace, in a neighborhood of the equilibrium, the unknown system, one output of which is the villi cell number, by its linear tangent system (see for example Perko [34]).

To justify the particular form adopted for this linear system, first consider that the villi population is not submitted to a renewal process from itself, so $\frac{dA}{dt}$ is not dependent on A; besides, the factor 1 between $\frac{dA}{dt}$ and $Z - Z_{eq}$ is justified by the fact that eliminated villi cells may be reasonably assumed to be compensated one for one by the flow of young cells from the crypts. In this respect, Z_{eq} is clearly the mean rate of mature cells which are eliminated in the intestinal lumen: 1400/day for a villus of 3500 cells, according to [21], hence the number of approximately 16500 cells per time unit (=1 h) and for an equilibrium villi population of (arbitrarily) 10^6 cells.

Second, the estimation of the coefficients on the second line $\left(\frac{dZ}{dt}\right)$ comes from 3 equations:

a. The equation giving the dampening coefficient over one period (T):

$$s = \exp\left(-\frac{\alpha}{2}T\right)$$

since $-\frac{\alpha}{2}$ is the real part of the eigenvalues of the linear system, the characteristic polynomial of which is $\lambda^2 + \alpha\lambda + \beta$ (and $s=\frac{1}{3}$ after estimation based on literature data [22]).

b. The equation giving the period of oscillations: $T = \frac{2\pi}{\omega}$, where ω is the imaginary part of the complex eigenvalues of the linear system, i.e.

$$\omega = \sqrt{\beta - \frac{\alpha^2}{4}}$$

(T=6 days after estimation based on published data[22]).

c. The equilibrium equation

$$\alpha Z_{\mathrm{eq}} + \beta A_{\mathrm{eq}} = \gamma.$$

Hence the values of α, β, γ

$$\alpha = -2\frac{\ln s}{T},\ \beta = \frac{4\pi^2 + (\ln s)^2}{T^2},\ \gamma = \alpha Z_{\mathrm{eq}} + \beta A_{\mathrm{eq}}$$

A.2. Gompertz model for tumor growth without treatment

In principle, as the Gompertz model is without treatment linear in $W=\ln B$: $\frac{dW}{dt} = a(W_{\max} - W)$, it should be possible to obtain the slope $-a$ and intercept $aW_{\max}$ by linear interpolation on a data set $\left(\ln B(t_i),\ \frac{\ln B(t_{i+1}) - \ln B(t_i)}{B(t_i)(t_{i+1}-t_i)}\right)$. But such an identification procedure requires points rather close to one another on the S-shaped curve, which was not the case in our laboratory data set that showed only three points per week.

So we used another procedure, eliminating the unreachable value $B_{\max}$, based on the equation $\frac{dW}{dt} = a(W_{\max} - W)$: since

$$W_{\max} - W(t) = \mathrm{e}^{-a(t-t_0)}(W_{\max} - W(t_0))$$

i.e. for all i

$$\ln B_{\max} - \ln B(t_i) = \mathrm{e}^{-a(t_i-t_0)} \ln \frac{B_{\max}}{B(t_0)}$$

$$\ln B_{\max} - \ln B(t_{i+1}) = \mathrm{e}^{-a(t_{i+1}-t_0)} \ln \frac{B_{\max}}{B(t_0)}$$

whence

$$\frac{\ln B(t_{i+2}) - \ln B(t_i)}{\ln B(t_{i+1}) - \ln B(t_i)} = \frac{\mathrm{e}^{-a(t_{i+2}-t_0)} - \mathrm{e}^{-a(t_i-t_0)}}{\mathrm{e}^{-a(t_{i+1}-t_0)} - \mathrm{e}^{-a(t_i-t_0)}}.$$

Given three consecutive times t_i, t_{i+1}, t_{i+2}, the first member is known, and the second is a rational fraction in $X=\mathrm{e}^{-24a}$, since any t_i is of the form t_0+24k_i, $k_i \in \mathbb{N}$. This gives a polynomial equation in X, which has always one root strictly between 0 and 1, the natural logarithm of which is identified as $-24a$. For this procedure to be efficient, it is necessary to choose three points in the middle part of the evolution curve, not too close to its beginning, where $\ln B(t)$ is almost constant, and not too far, where other phenomena, e.g., linked to neoangiogenesis, may complicate the picture. This usually left hardly more than three points in our laboratory data set, e.g., measures at days 8, 9 and 12 on untreated animals, or days 16, 19 and 21 on treated animals.

We estimated $G = a\ln\frac{B_{\max}}{B(t_0)} = \frac{dB(t_1)}{B(t)dt}\big|_{t=t_0}$ by $\frac{B(t_1)-B(t_0)}{B(t_0)(t_1-t_0)}$ i.e., on the initial part of the curve, where $B(t_1)-B(t_0)$ is small, but non-zero, whence the determination of $B_{\max}=B(t_0).\mathrm{e}^{G/a}$. These primary estimations were then used as initial values for curve fitting algorithms, by using a least mean square procedure on each individual animal tumor growth evolution curve.

Only one pair of values (a=0.015, $B_{\max}=5.3\times B(t_0)$) was retained for further simulations and optimization procedures. These values correspond to a concave growth curve, since for parameter estimations we have focused on the fast growing part of each curve.

It means that we have in fact simulated an efficient treatment beginning at an advanced stage of tumor growth.

A.3. Pharmacodynamics

As mentioned above, the jejunal toxicity function ($f(C)$) could not be identified, and was arbitrarily set as yielding likely curves for the enterocyte population, with levels not under 10% of the equilibrium value for the drug doses in use at our laboratory. In the absence of data on the subject, for instance, 40% of villi population depletion was set to represent moderate toxicity, and 60% severe toxicity.

For the anti-tumor therapeutic efficacy function ($g(D)$), tumor size evolution curves under treatment were available. Animals which had previously been synchronized to an environmental regimen of 12 h of light alternating with 12 h of darkness and had received subcutaneous inoculation of Glasgow Osteosarcoma cells were treated with the same daily dose of oxaliplatin, according to a procedure described in [11] (where one can find that another daily dose of 5.25 mg/kg/d was also used, confirming the optimality of the 15 HALO injection phase). The treatment consisted of a bolus of 4 mg of oxaliplatin injected in the retroorbital venous sinus on four consecutive days with different groups of animals each one being treated consistently at one of six different HALO time points (each differing by 4 HALO from another). We could then compute the dynamics of the oxaliplatin concentration and therapeutic effect based on our model, as a function of its maximal value $2H$ (D_{T50} and γ_T being fixed respectively as 10 and 1, to obtain $g(D)\approx\frac{H}{D_{\mathrm{T50}}}D$ for current levels of variable D, a quasi-linear behavior), and compare these calculations with the experimental curves. We started from the linear relation

$$\frac{dW}{dt} = -aW + aW_{\max} - g(D)$$

where $W=\ln B$; on integration, this becomes:

$$W(t) = W_{\max} + e^{at}(W_0 - W_{\max}) - e^{-at}\int_0^t \frac{HD(u)e^{au}}{D_{T50}+D(u)}\left\{1+\cos 2\pi\frac{(u-\varphi_T)}{24}\right\}du$$

whence

$$H = \frac{e^{at}\ln\frac{B_{\max}}{B(t)} - \ln\frac{B_{\max}}{B_0}}{\int_0^t \frac{e^{au}D(u)}{D_{T50}+D(u)}\left\{1+\cos 2\pi\frac{(u-\varphi_T)}{24}\right\}du}.$$

The integral was evaluated between time 0, representing the time of the last bolus of a series of four injections, on days 5, 6, 7 and 8 after tumor inoculation (the tumor being palpable on day 5), and other subsequent times, evenly spaced by multiples of 24 h. For instance, with $t=0$ corresponding to the last injection on day 8, time t for the upper bound of the integral was 13×24 h, corresponding to a measure on day 21, at the same given HALO.

Each bolus was injected at the same HALO for the same animal, and consisted of a unique dose (per day) of 4 mg/kg oxaliplatin (60 μg of free platinum for a 30 g mouse). Each bolus was taken as an initial condition $P_0=60$ μg, for the first equation, whence $D(t)$ (drug concentration in the tumor):

$$D(t) = \frac{P_0}{\lambda}\left(1+e^{-24v}+e^{-48v}+e^{-72v}\right)e^{-vt}.$$

In order to assess comparable data, we evaluated a and $B_{\max}$ on the same mouse chosen for the evaluation of H, but at the end of the tumor size curve, when drug concentration in the tumor was almost zero. As stated earlier, there were so large inter-individual differences in the evaluation of the Gompertz parameters G and $B_{\max}$ that we preferred this procedure, specifically for the evaluation of parameter H, rather than evaluating G and $B_{\max}$ on curves without treatment for other mice.

Based on these computations for the evaluation of H on different mice subject to oxaliplatin injections, we eventually used an H value of 2, which allowed us to qualitatively compare treatments in an effective way in model simulations.

The time difference $\Delta\varphi$ of approximately 6 h between the phase φ_T of maximal therapeutic effect and the optimal peak infusion phase φ_I (for a bolus, beginning and peak times are the same) may be obtained as follows.

Suppose a bolus of drug is injected at $t=0$, giving rise to an initial concentration P_0. Then by straightforward integration, plasma concentration will be $P(t)=P_0e^{-\lambda t}$ and tissue concentration, $D(t)=P_0=\frac{e^{-vt}-e^{-\lambda t}}{\lambda-v}\approx\frac{P_0}{\lambda}e^{-vt}$, since $v\ll\lambda$.

Replacing the pharmacodynamic function (with $\gamma_T=1$): $g(D)=H\frac{D}{D_{T50}+D}\left\{1+\cos\frac{2\pi}{24}(t-\varphi_T)\right\}$ by a linear approximation in D, $g(D)=H_0D\left\{1+\cos\frac{2\pi}{24}(t-\varphi_T)\right\}$, we have $g(D(t))=H_0\frac{P_0}{\lambda}e^{-vt}\left\{1+\cos\frac{2\pi}{24}(t-\varphi_T)\right\}$.

On integration between 0 and 24 h of the equation

$$\frac{d}{dt}\ln(B/B_{\max}) = \frac{dB}{Bdt} = -a.\ln(B/B_{\max}) - g(D)$$

we obtain

$$\ln(B(24)/B_{\max}) = \ln(B(0)/B_{\max})e^{-24a} - e^{-24a}\int_0^{24} H_0\frac{P_0}{\lambda}e^{(a-v)t} \times\left\{1+\cos\frac{2\pi}{24}(t-\varphi_T)\right\}dt$$

and we want to know for which value of φ_T this last integral takes its maximum: this value of φ_T will be the delay between the optimal injection time (known from experimental observations, here assumed to be zero) and the tissue optimal anti-tumor efficacy time φ_T. This maximum will be obtained when its derivative with respect to φ_T is zero, i.e., when

$$\int_0^{24} e^{(a-v)t}\left\{\sin\frac{2\pi}{24}(t-\varphi_T)\right\}dt = 0$$

which by simple computation is the case if and only if

$$(a-v)\sin\frac{2\pi}{12}\varphi_T + \frac{\pi}{12}\cos\frac{\pi}{12}\varphi_T = 0$$

leading to

$$\varphi_T = \frac{12}{\pi}\ \text{Arc tan}\ \frac{\pi}{12(v-a)}$$

with $v=0.03$ and $a=0.015$, this value is approximately 5.78 h, for which value of φ_T the second derivative

$$-\frac{2\pi}{24}\int_0^{24} e^{(a-v)t}\left\{\cos\frac{2\pi}{24}(t-\varphi_T)\right\}dt$$

of the integral with respect to φ_T is easily seen to be negative, showing that the integral actually reaches a maximum for this value of φ_T. Hence if the optimal injection time has been approximately determined as 15 HALO, then this means that $\varphi_T\approx 21$ HALO.

Acknowlegments

I am gratefully indebted to Michael Smolensky who did not spare his time in helping to revise the manuscript.

References

[1] A. Goldbeter, A model for circadian oscillations in the *Drosophila* period protein (PER), Proc. R. Soc. Lond. B 261 (1995) 319–324.
[2] A. Goldbeter, Computational approaches to cellular rhythms, Nature 420 (2002) 238–245.
[3] J.-C. Leloup, A. Goldbeter, Toward a detailed computational model of the mammalian circadian clock, Proc. Nat. Acad. Sci. 100 (12) (2003) 7051–7056.
[4] L. Fu, H. Pelicano, J. Liu, P. Huang, C.C. Lee, The circadian gene Period2 plays an important role in tumor suppression and DNA damage response in vivo, Cell 111 (2002) 41–50.
[5] M. Rosbash, J. Takahashi, The cancer connection, Nature 420 (2002) 373–374.
[6] L. Fu, C.C. Lee, The circadian clock: pacemaker and tumor suppressor, Nature Reviews 3 (2003) 351–361.
[7] F. Lévi, Cancer chronotherapeutics, Special Issue of Chronobiology International, 19 (1), 2002.

[8] B. Hecquet, Modélisation pour une chronopharmacologie, Pathologie-Biologie 35 (6) (1986) 937–941.
[9] J. Clairambault, D. Claude, E. Filipski, T. Granda, F. Lévi, Toxicité et efficacité antitumorale de l'oxaliplatine sur l'ostéosarcome de Glasgow induit chez la souris: un modèle mathématique, Pathologie-Biologie 51 (2003) 212–215.
[10] F. Lévi, B. Perpoint, et al., Oxaliplatin activity against metastatic colorectal cancer. A phase II study of 5-day continuous venous infusion at circadian rhythm modulated rate, Eur. J. Cancer 29A (9) (1993) 1280–1284.
[11] T.G. Granda, R.M. D'Attino, E. Filipski, et al., Circadian optimization of irinotecan and oxaliplatin efficacy in mice with Glasgow osteosarcoma, Brit. J. Cancer 86 (2002) 999–1005.
[12] N.A. Boughattas, F. Lévi, et al., Circadian rhythm in toxicities and tissue uptake of 1,2-diamminocyclohexane(*trans*-1)oxaloplatinum(II) in mice, Cancer Research 49 (1989) 3362–3368.
[13] C. Haurie, D.C. Dale, M.C. Mackey, Cyclical neutropenia and other hematological disorders: a review of mechanisms and mathematical models, Blood 92 (8) (1998) 2629–2640.
[14] F. Lévi, G. Metzger, C. Massari, G. Milano, Oxaliplatin: pharmacokinetics and chronopharmacological aspects, Clin. Pharmacokinet. 38 (2000) 1–21.
[15] S. Faivre, D. Chan, R. Salinas, B. Woynarowska, J.M. Woynarowski, DNA strand breaks and apoptosis induced by oxaliplatin in cancer cells, Biochemical pharmacology 66 (2003) 225–237.
[16] S.G. Chaney, S.L. Campbell, E. Bassett, Y.B. Wu, Recognition and processing of cisplatin-and oxaliplatin-DNA adducts, Clin. Rev. Oncol. Hematol. 53 (2005) 3–11.
[17] D.M. Kweekel, H. Gelderblom, H.-J. Guchelaar, Pharmacology of oxaliplatin and the use of pharmacogenomics to individualize therapy, Canc. Treatment Rev. 31 (2005) 90–105.
[18] D. Wang, S.L. Lippard, Cellular processing of platinum anticancer drugs, Nature Rev. Drug Discovery 4 (2005) 307–320.
[19] M. Mishima, G. Samimi, A. Kondo, X. Lin, S.B. Howell, The cellular pharmacology of oxaliplatin resistance, Eur. J. Cancer 38 (2002) 1405–1412.
[20] N.A. Boughattas, B. Hecquet, C. Fournier, B. Bruguerolle, A. Trabelsi, K. Bouzouita, B. Omrane, F. Lévi, Comparative pharmacokinetics of oxaliplatin (L-OHP) and carboplatin (CBDCA) in mice with reference to circadian dosing time, Biopharm Drug Dispos. 15 (1994) 761–773.
[21] C.S. Potten, M. Loeffler, Stem cells: attributes, cycles, spirals, pitfalls and uncertainties, Lessons Crypt. Dev. 110 (1990) 1001–1020.
[22] N. Wright, M. Alison, The Biology of Epithelial Cell Populations, vol.2, Clarendon Press, Oxford, 1984, pp. 842–869, chap.23.
[23] L. Edelstein-Keshet, Mathematical Models in Biology, McGraw-Hill, New York, 1988, pp. 210–270.
[24] M. Gyllenberg, G.F. Webb, Quiescence as an explanation of Gompertzian tumor growth, Growth, Development and Aging 53 (1989) 25–33.
[25] M. Gyllenberg, G.F. Webb, A nonlinear structured population model of tumor growth with quiescence, J. Math. Biol. 28 (1990) 671–694.
[26] T.L. Jackson, H.M. Byrne, A mathematical model to study the effects of drug resistance and vasculature on the response of solid tumors to chemotherapy, Math. Biosci. 164 (2000) 17–38.
[27] J.A. Sherratt, M.A.J. Chaplain, A new mathematical model for avascular tumour growth, J. Math. Biol. 43 (2001) 291–312.
[28] P. Hahnfeldt, D. Panigrahy, J. Folkman, L. Hlatky, Tumor development under angiogenic signaling: a dynamical theory of tumor growth, treatment response, and postvascular dormancy, Cancer Research 59 (1999) 4770–4775.
[29] A. Ergun, K. Camphausen, L.M. Wein, Optimal scheduling of radiotherapy and angiogenic inhibitors, Bull. Math. Biol. 65 (2003) 407–424.
[30] J.H. Goldie, A.J. Coldman, A mathematic model for relating the drug sensitivity of tumors to their spontaneous mutation rate, Cancer Treat. Rep. 63 (1979) 1727–1733.
[31] N.F. Britton, N.A. Wright, J.D. Murray, A mathematical model for cell population kinetics in the intestine, J. Theor. Biol. 98 (1982) 531–541.
[32] X.M. Li, G. Metzger, E. Filipski, G. Lemaigre, F. Lévi, Modulation of nonprotein sulphydryl compounds rhythm with buthionine sulphoximine: relationship with oxaliplatin toxicity in mice, Arch. Toxicol. 72 (1998) 574–579.
[33] M.H. Hastings, A.B. Reddy, E.S. Maywood, A clockwork web: circadian timing in brain and periphery, in health and disease, Nat. Rev./Neurosci. 4 (2003) 649–661.
[34] L. Perko, Differential Equations and Dynamical Systems, 2nd edition, Springer, 1996, pp. 119–129.
[35] L.E. Scheving, E.R. Burns, J.E. Pauly, T.H. Tsai, Circadian variations in cell division of the mouse alimentary tract, bone marrow and corneal epithelium, Anat. Rec. 191 (1978) 479–486.
[36] A. Iliadis, D. Barbolosi, Optimising drug regimens in cancer chemotherapy by an efficacy-toxicity mathematical model, Computers Biomed. Res. 33 (2000) 211–226.
[37] A. Iliadis, D. Barbolosi, Optimising drug regimens in cancer chemotherapy: a simulation study using a PK–PD model, Computers Biol. Med. 31 (2001) 157–172.
[38] C. Basdevant, J. Clairambault, F. Lévi, Optimisation of time-scheduled regimen for anti-cancer drug infusion, Math. Model. Numer. Anal. 39 (6) (2005) 1069–1086.
[39] D.B. Forger, R.E. Kronauer, Reconciling mathematical models of biological clocks by averaging on approximate manifolds, SIAM J. Appl. Math. 62 (4) (2002) 1281–1296.
[40] F.A. Levi, N. Tubiana-Mathieu, C. Focan, C. Brézault-Bonnet, B. Coudert, C. Carvalho, D. Genet, S. Giacchetti, M.-A. Lentz, B. Baron, First line infusion of 5-fluorouracil, leucovorin and oxaliplatin for metastatic colorectal cancer: 4-day chronomodulated (FFL410) versus 2-day FOLFOX2, A Multicenter Randomized Phase III Trial of the Chronotherapy Group of the European Organization for Research and Treatment of Cancer (EORTC 05963). ASCO Meeting Abstracts, 22, 2004, p. 3526.
[41] J.C. Panetta, A mathematical model of drug resistance: heterogeneous tumors, Math. Biosci. 147 (1998) 41–61.
[42] F. Kozusko, P.H. Chen, S.G. Grant, B.W. Day, J.C. Panetta, A mathematical model of in vitro cancer cell growth and treatment with the antimitotic agent curacin A, Math. Biosci. 170 (2001) 1–16.
[43] J. Clairambault, P. Michel, B. Perthame, Circadian rhythm and tumour growth, C. R. Acad. Sci. (Paris) 342 (1) (2006) 17–22.
[44] J.C. Panetta, A mathematical model of breast and ovarian cancer treated with Paclitaxel, Math. Biosci. (1997) 89–113.
[45] J.L. Boldrini, M.I.S. Costa, Therapy burden, drug resistance, and optimal treatment regimen for cancer therapy, IMA J. Math. Appl. Med. Biol. 17 (2000) 33–51.